Conformational Analysis of Pseudocyclic Hexapeptides Based on Quantitative Circular Dichroism (CD), NOE, and X-ray Data. The Pure CD Spectra of Type I and Type II β-Turns

András Perczel,[§] Miklos Hollósi,[§] Bruce M. Foxman,[‡] and Gerald D. Fasman*,[†,‡]

Contribution from the Graduate Departments of Biochemistry and Chemistry, Brandeis University, Waltham, Massachusetts 02254-9110, and Institute of Organic Chemistry, Eötvös University, H-1518 Budapest 112, P.O. Box 32, Hungary. *Received May 3, 1991*

Abstract: The β-turn (type I and type II) is the third frequently found structural unit involved in the 3D structure of globular proteins, in addition to the two major secondary structural elements, the α-helix and the β-pleated sheet. Despite several theoretical and empirical efforts, the circular dichroism (CD) spectra of the pure type I and type II β-turns are still not established beyond doubt. Even though considerable information is known about the CD spectra of the α-helix and β-sheet, the lack of knowledge concerning the β-turn pure component spectra renders the estimation of global secondary structure of proteins rather inaccurate. To obtain more precise information about β-turn conformations, cyclo[Gly-Pro-Ser(O^{t}Bu)-Gly-(δ)Ava] (**2**) and cyclo[Gly-Pro-Ser(OH)-Gly-(δ)Ava] (**3**) were synthesized, and their CD spectra were studied. The object of the conformational analysis reported herein was to determine the crystalline state geometry of **2** as well as the solution conformations of **2** and **3** by NMR. In the crystal, **2** was found to adopt an "ideal" type I β-turn, encompassing the -Pro-Ser- dipeptide. *Quantitative nuclear Overhauser effect* measurements yielded interproton distances and the conformational ratios of **2** and **3**. NOE distances so obtained were compared to values determdined by X-ray diffraction, while solution conformational ratios were compared with the results of a *quantitative CD interpretation*. Using a recently developed algorithm, the conformational deconvolution of the measured CD spectra yielded the pure component CD curves of type I and type II β-turns. The NOE data confirmed the ratios of the CD component curves of the two major β-turn types. These results will facilitate the conformational determination of globular proteins on the basis of their CD spectra.

Introduction

Numerous cyclic hexapeptides have been synthesized in order to study the structure–activity relationship in polypeptide analogues of hormones, inhibitors, antibiotics, toxins, etc.[3] As well as being investigated for their biochemical significance, several of these peptides have been thoroughly studied for their conformational properties.[4] By contrast, only a smaller number of cyclic hexapeptide derivatives have been designed especially for conformational investigations, although their cyclic structures were known to incorporate β- and/or γ-turns. Although NMR is gaining acceptance as the tool of choice for secondary structure determination, circular dichroism (CD) spectroscopy is still a widely used tool for the structural determination of polypeptides and proteins because of its high conformational sensitivity[5] and its small sample size requirement. The CD spectrum of a polypeptide chain is mainly determined by the *spatial arrangement of the chromophores* (amide groups) around the chiral centers (C^α atoms of the amino acids). Therefore a peptide designed for the investigation of its conformational CD properties, must include the correct number of chromophores as well as having a degree of "conformational rigidity".

An estimation of the secondary structural elements of a protein may be obtained by the analysis of its CD spectrum (below 240 nm).[6a] The first effort along these lines was the study of Greenfield and Fasman.[6b] The analysis is generally based on the determination and empirical correlation of measured CD spectra with major secondary structural elements. The linear combination of the weighted "pure CD component" curves can yield the measured CD spectra of complex structures. Besides the two major secondary structural elements composed of recurring conformational subunits such as helices (α-helix, 3_{10} helix, and π-helix) ($\phi_1 = -60° \pm 30°$, $\psi_1 = -60° \pm 30°$) and the different forms of β-pleated sheets ($\phi_1 = -150° \pm 30°$, $\psi_1 = +150° \pm 30°$), a third frequently found typical structural unit in globular proteins is the β-turn conformation.[7] This third secondary structure is made up of subunits of *nonrecurring* conformations. In globular proteins type I and type II β-turns occur typically with the following backbone torsion angles ($\phi_{i+1}^{typeI} = -60° \pm 30°$, $\psi_{i+1}^{typeI} = -30° \pm 30°$, $\phi_{i+2}^{typeI} = -90° \pm 30°$, $\psi_{i+2}^{typeI} = 0° \pm 30°$) ($\phi_{i+1}^{typeII} = -60° \pm 30°$, $\psi_{i+1}^{typeII} = +120° \pm 30°$, $\phi_{i+2}^{typeII} = +80° \pm 30°$, $\psi_{i+2}^{typeII} = 0° \pm 30°$), respectively.[7b] (For a definition and for ϕ,ψ torsion angle values of other less frequently observed β-turns, see the review of Smith and Pease[7]). Although several theoretical and empirical approaches have been made, the CD spectra of the pure type I and type II β-turns are still not established beyond doubt. Considerable information is known about the CD spectra of the α-helix and β-sheets, but the lack of knowledge concerning the β-turn pure component spectra renders the estimation of the global secondary protein structure rather inaccurate and unreliable.[6a]

On the basis of Woody's theoretical approach,[8] performed on a triamide chiral unit in a β-turn conformation (Ac-Ala-Ala-$NHCH_3$), it is known that the backbone dihedral angles (ϕ_1, ψ_1, ϕ_2, ψ_2) have a basic influence on the $n\pi^*$ and $\pi\pi^*$ rotational strengths. Woody distinguished four classes (A, B, C, and D) of CD spectral patterns for β-turns.[9] Despite the fact that such

* Author to whom correspondence should be sent.
† Rosenfield Professor of Biochemistry.
‡ Brandeis University.
§ Eötvös University.

(1) This research was generously supported in part by a grant from the National Science Foundation (G.D.F., NSF No. DMB-8512570) and a National Scientific Research Foundation Grant (M.H., OTKA No. 1-600-2-88-1-591, Hungary).

(2) Abbreviations: Aaa = alpha amino acid, (δ)Ava = 5-amino valeric acid, (ε)Aca = 6-aminocapric acid, CD = circular dichroism, CI = chemical ionization, COSY = correlated spectroscopy, EI = electric ionization, NOE = nuclear Overhauser effect, NOESY = nuclear Overhauser and exchange spectroscopy, CCA = convex constraint analysis, MD = molecular dynamics.

(3) Rose, G. D.; Gierasch, L. M.; Smith, J. A. *Adv. Prot. Chem.* **1985**, *37*, 1.

(4) (a) Bruch, M. D.; Noggle, J. H.; Gierasch, L. M. *J. Am. Chem. Soc.* **1985**, *107*, 1400. (b) Kessler, H.; Anders, U.; Schudok, M. *J. Am. Chem. Soc.* **1990**, *112*, 5908. (c) Gierasch, L. M.; Deber, C. M.; Madison, V.; Niu, C.-H.; Blout, E. R. *Biochemistry* **1981**, *20*, 4730.

(5) Neumann, N.; Snatzke, G. In *Proteins: Form and Function*; Bradshaw, R. A., Purton, M., Eds., Elsevier Trends Journals: Cambridge, England, 1990; p 107.

(6) (a) Yang, J. T.; Wu, C.-S. C.; Martinez, H. M. In *Methods in Enzymology*; Academic Press: New York, 1986; Vol. 130, p 208. (b) Greenfield, N. J.; Fasman, G. D. *Biochemistry* **1969**, *8*, 4108.

(7) (a) Smith, J. A.; Pease, L. G. *CRC Crit. Rev. Biochem.* **1980**, *8*, 315. (b) Chou, P.; Fasman, G. D. *J. Mol. Biol.* **1977**, *115*, 135. (c) Bush, A. C.; Sarkar, S. K.; Kopple, D. K. *Biochemistry* **1978**, *17*, 4951.

(8) (a) Woody, R. W. *Biopolymers* **1978**, *17*, 1451. (b) Woody, R. W. In *The Peptides* 7; Hruby, V. J., Ed.; Academic Press: New York, 1985; p 15.

0002-7863/91/1513-9772$02.50/0

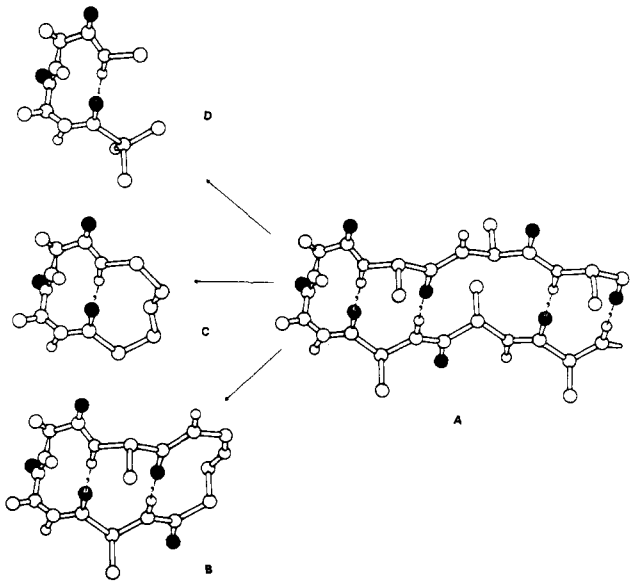

Figure 1. The schematic representation of the three different types of β-turn models: (A) a β-turn at the terminus of an antiparallel β-pleated sheet, (B) cyclo[Gly-Xxx-Yyy-Gly-(δ)Ava] type models, (C) cyclo-[Xxx-Yyy-(ε)Aca] type models, and (D) Piv-Xxx-Yyy-$NHCH_3$ and Boc-Xxx-Yyy-$NHCH_3$ type models.

patterns have already been observed in some linear and cyclic peptides, there is not an unambiguous correlation the β-turn types and the above spectral classes.

A systematic investigation has been initiated in order to obtain the CD properties of β-turns using carefully designed linear and bridged cyclopeptide models.[9-14] Different models of β-turns in peptides have been synthesized (see Figure 1) by varying the size and the amino acid content of these models. On the basis of the statistical analysis of several β-turn fragments of proteins whose structure was determined by X-ray diffraction, several -Xxx-Yyy-dipeptides were incorporated into the turn of these models and investigated using different "mobility-decreasing" factors.[9-14] The interesting CD spectrum of cyclo[Ala-Ala-(ε)Aca] initiated studies of three different types of β-turn models, all containing only two chiral residues (cf. Figure 1). The -Pro-Ser- subunit is not only a frequently found amino acid pair in β-turns of globular proteins [e.g., elastase (at residues 28,29), subtilisin BPN' (at residues 52,53 and 172,173), hemoglobin (at residues 32,33)] but also can be the target of post-translational modifications (O-glycosylation and/or O-phosphorylation) related again with β-turn conformations.[15,16] The design of the model with the composition of cyclo[Gly-Pro-Ser-Gly-(δ)Ava] (**3**) was guided by several factors aimed at "optimizing" the CD properties of the implanted β-turn structure.[9] Chiral amino acids were introduced only in the central part of the β-turn (positions i+1 and i+2), while glycines were used elsewhere (positions i and i+3) and the hairpin subunit was bridged by a suitable nonchiral δ-amino acid, to yield a peptide backbone having a favorable hexapeptide size. The conformational mobility was decreased by fixing the ϕ_{i+1} torsion angle at a favorable β-turn value (by the pyrrolidine ring of the proline residue) and by the protection of the serine side chain in the form of a bulky *tert*-butyl ether. The presence of the two flexible glycine units made possible the investigation of the role of intramolecular H-bond (1-10) in β-turn stability and the additional stabilizing effect of the following (1-14) H-bond.

The object of the conformational analysis reported herein was to establish a complete conformation analysis of the pure component CD spectra of β-turns, using the crystal state geometry of cyclo[Gly-Pro-Ser(O^{t}Bu)-Gly-(δ)Ava] (**2**) as well as the solution conformations of **2** and cyclo[Gly-Pro-Ser(OH)-Gly-(δ)Ava] (**3**) obtained by NMR.

Table I. ^{13}C Chemical Shifts at 20 °C of HCl·H(δ)Ava-Gly-Pro-Ser(O^{t}Bu)-Gly-OH (**1**) in DMSO-d_6, Cyclo[(δ)Ava-Gly-Pro-Ser(O^{t}Bu)-Gly] (**2**) in CD_3CN, and Cyclo[(δ)Ava-Gly-Pro-Ser-Gly] (**3**) in CD_3CN

		$trans_{Pro}$	**1**	cis_{Pro}	**2**[a]	**3**
Gly	α	41.53		41.06	42.03	42.24
Gly	α	41.87		41.69	42.90	42.87
Pro	α	60.02		58.93	62.38	62.17
	β	29.37		29.84	29.73	29.61
	γ	26.73		26.66	24.94	24.83
	δ	46.25		47.03	47.08	47.23
Ser	α	53.57		53.67	53.81	56.20
	β	61.79		61.89	61.51	62.13
Ava	α	34.71		34.61	35.05	35.04
	β	22.40		22.25	22.85	22.79
	γ	24.45		24.48	28.42	28.40
	δ	38.50		38.58	37.20	37.62
C'	1	172.01		171.84	173.93	174.68
	2	171.53		171.35	171.88	172.36
	3	171.01		170.93	170.54	171.47
	4	169.43		169.31	170.56	170.40
	5	167.61		167.40	176.71	169.84

[a] **2** in DMSO-d_6 contains <10% *cis*-Proline.

Experimental Section

Synthesis. The linear precursor of **2**, the HCl·H-(δ)Ava-Gly-Pro-Ser(O^{t}Bu)-Gly-OH (**1**), was prepared as described earlier by Hollősi et al.[9] and characterized via ^{13}C NMR data (cf. Table I). Cyclization was performed as described earlier[9] as well as using benzotriazol-1-yloxy-tris(dimethylamino)phosphonium hexafluorophosphate[17a,b] (Aldrich). The side chain protected cyclo[Gly-Pro-Ser(O^{t}Bu)-Gly-(δ)Ava] (**2**) was crystallized from absolute ethanol and studied by mass spectroscopy (CI and EI), by ^{13}C and ^1H NMR (cf. Tables I, II, and III (see supplementary material for Table III)). Cleavage of the protecting group was achieved by dissolving **1** in F_3CCOOH (TFA) (Aldrich) at 0 °C for 30 min. The solvent was removed under vacuum, and the crude cyclo-[Gly-Pro-Ser-Gly-(δ)Ava] (**3**) was washed several times with dried ether and then crystallized from absolute ethanol. The cyclic peptide was finally analyzed by HPLC and analyzed by mass spectroscopy (EI and CI methods) as well as NMR methods (cf. Tables I, IV, and V (see supplementary material for Table V)). The HPLC was run on Ultrasphere-ODS 5-μ column (4.6 × 250 mm ALTEX) using the gradient method (A = 1000 mL of H_2O plus 1 mL of TFA, B = 1000 mL of CH_3CN plus 1 mL of TFA) at a flow rate of 1 mL/min yielding a k' (for **2**) = 6.1 and k' (for **3**) = 2.95; k' was calculated as usual $k' = (t - t_0)/t_0$. (Detection was performed at 214 nm.)

X-ray Measurement. Structure Determination of cyclo[(δ)-Ava-Gly-Pro-Ser(O^{t}Bu)-Gly]·$2H_2O$. Single crystals were grown by slow cooling of an ethyl acetate solution. The crystal was mounted on a Pyrex fiber, transferred to a Supper No. 455 goniometer, and optically centered on a Syntex $P2_1$ diffractometer. Operations were performed as described previously.[18] The analytical scattering factors of Cromer and Waber were used; real and imaginary components of anomalous scattering were included in the calculations.[19] The structure was solved using SHELXS-

(9) Hollősi, M.; Köver, K. E.; Holly, S.; Radics, L.; Fasman, G. D. *Biopolymers* **1987**, *26*, 1555.
(10) Perczel, A.; Hollősi, M.; Fülöp, V.; Kalmán, A.; Sándor, P.; Fasman, G. D. *Biopolymers* **1990**, *30*, 763.
(11) Aubry, A.; Ghermani, N.; Marraud, M. *Int. J. Peptide Protein Res.* **1984**, *23*, 113.
(12) Marraud, M.; Aubry, A. *Int. J. Peptide Protein Res.* **1984**, *23*, 123.
(13) Bandekar, J.; Evans, D. J.; Krimm, S.; Leach, S. J.; Lee, S.; McQuire, J. R.; Minasian, E.; Némethy, G.; Pottle, M. S.; Scheraga, H. A.; Stimson, E. R.; Woody, R. W. *Int. J. Peptide Protein Res.* **1982**, *19*, 187.
(14) DesLauriers, R.; Evans, D. J.; Leach, S. J.; Meinwald, Y. C.; Minasian, E.; Némethy, G.; Rea, I. D.; Scheraga, H. A.; Somorjai, R. L.; Stimson, E. R.; Van Nispen, J. W.; Woody, R. W. *Macromolecules* **1981**, *14*, 985.
(15) Hollősi, M.; Perczel, A.; Fasman, G. D. *Biopolymers* **1990**, *29*, 1549.
(16) Frank, A. N. *CRC Crit. Rev. Biochem.* **1984**, *16*, 51. Stradley, S. J.; Rizo, J.; Bruch, M. D.; Stroup, A. N.; Gierasch, L. M. *Biopolymers* **1990**, *29*, 263.
(17) (a) Castro, B.; Dormoy, J. R.; Evin, G.; Selve, C. *Tetrahedron Lett.* **1975**, *1219*, 2. (b) Castro, B.; Evin, G.; Selve, C.; Seyer, R. *Synthesis* **1977**, *6*, 413.
(18) Foxman, B. M. *Inorg. Chem.* **1978**, *17*, 1932. Foxman, B. M.; Mazurek, H. *Inorg. Chem.* **1979**, *18*, 113.
(19) *International Tables for X-ray Crystallography*; Kynoch Press: Birmingham, England, 1974; Vol. IV, pp 99, 148.

Table II. 300-MHz ^{1}H NMR Data on Cyclo[(δ)Ava-Gly-Pro-Ser(O^{t}Bu)-Gly] (**2**) in CD_3CN

	Gly_1	Pro	Ser	Gly_2	(δ)Ava	
	(1 H, dd)		(1 H, dd)	(1 H, dd)	(1 H, dd)	
$\delta NH^{(ppm)}$	7.01		6.94	7.48	6.61	$\delta NH^{(ppm)}$
	(1.10)[a]		(1.21)	(1.15)	(1.73)	
$\delta H^{\alpha(ppm)}$	4.08	4.22	4.39	4.15	3.26	$\delta H^{\delta(ppm)}$
	3.96	(1.24)	(2.07)	3.42	3.23	
	(0.73)			(0.84)	(0.72)	
		(1 H, m)	(1 H, dd)		(2 H, m)	
$\delta H^{\beta(ppm)}$		2.20	3.71		1.57	$\delta H^{\gamma(ppm)}$
		1.83	3.61		1.46	
		(1.26)	(0.74)		(0.65)	
$^3J_{NH-\alpha H}$	5.4[b]		9.1	2.4		$^3J_{HN-\delta H}$
	5.6			5.3		
$^3J\alpha_H-\beta_H$		6.1	5.8		1.54	$\delta H^{\beta(ppm)}$
		8.9	3.8		(0.63)	
$^2J\alpha_H-\alpha_H$	17.5			16.8	2.26	$\delta H^{\alpha(ppm)}$
					2.20	
					(1.28)	
δH$^\gamma$ (ppm) of Pro 1.91, 1.98 (1.25)						
δH$^\delta$ (ppm) of Pro 3.58, 3.62 (0.76)						

[a] T_1 relaxation times. [b] Coupling constants are given in hertz.

Table IV. 300-MHz ^{1}H NMR Data on Cyclo[(δ)Ava-Gly-Pro-Ser(OH)-Gly] (**3**) in CD_3CN

	Gly_1	Pro	Ser	Gly_2	(δ)Ava	
	(1 H, dd)		(1 H, d)	(1 H, dd)	(1 H, dd)	
$\delta NH^{(ppm)}$	7.12		7.52	7.69	7.03	$\delta NH^{(ppm)}$
	(0.79)[a]		(0.75)	(0.74)	(0.67)	
	(1 H, dd)	(1 H, dd)	(1 H, ddd)	(1 H, dd)	(1 H, m)	
$\delta H^{\alpha(ppm)}$	4.17	4.23	4.28	4.15	3.27	$\delta H^{\delta(ppm)}$
	3.81	(0.61)	(1.47)	3.48	3.09	
	(0.52)			(0.53)	(0.45)	
		(1 H, m)	(1 H, dd)		(2 H, m)	
$\delta H^{\beta(ppm)}$		2.21	3.85		1.49	$\delta H^{\gamma(ppm)}$
		1.93	3.77		1.38	
		(0.51)	(0.48)		(0.41)	
$^3J_{HN-\alpha H}$	4.6[b]			3.5	5.6	$^3J_{HN-\delta H}$
			7.4			
	4.6			7.9	5.6	
$^3J_{\alpha H-\beta H}$		6.2			1.52	$\delta H^{\beta(ppm)}$
		9.1			(0.42)	
$^2J_{\alpha H-\alpha H}$	15.8			16.8	2.25	$\delta H^{\alpha(ppm)}$
					1.94	
					(0.54)	
δH$^\gamma$ (ppm) of Pro 1.94, 1.93						
δH$^\delta$ (ppm) of Pro 3.72, 3.53 (0.49)						

[a] T_1 relaxation times. [b] Coupling constants are given in hertz.

86;[20] all other computational work was carried out on a VAX 8650 computer using the Enraf-Nonius SDP software package.[21] At the conclusion of least-squares refinement of positional and anisotropic thermal parameters for all non-hydrogen atoms (H atoms included as fixed contributions to F_c), $R = 0.040$ and $R_w = 0.045$. The absolute configuration was established by reference to the *S*-proline residue. Details of the structure analysis, in outline form, are presented in Table VI. Atomic coordinates are listed in Table VII. Atomic displacement parameters, molecular geometry, calculated hydrogen atom coordinates, torsion angles, and structure factors are available as supplementary material. Observed hydrogen bonds are reported in Table VIII. Two additional single crystals of **2** were grown, one from CD_3CN and one from H_2O-saturated EtOAc are identical. These latter two crystals were subjected to a unit cell and space group determination on the $P2_1$ diffractometer. This determination showed that the crystals grown from CD_3CN and H_2O–EtOAc were identical to the crystal used for the X-ray structure determination.

NMR Measurement. ^{1}H and ^{13}C NMR measurements were performed on a VARIAN XL-300 spectrometer at ambient temperature (25 °C). **2** and **3** were dissolved in CD_3CN or in CD_3CN/DMSO (1:4) and degassed using at least ten freeze–pump–thaw cycles. Assignments of ^{1}H signals were made with 2D decoupling experiments on **2** and **3**. Correlated spectroscopy (COSY) data consisted of 256 t_1 increments with a relaxation delay of 1 s. The 2D J resolved spectra were recorded with a total of 16 or 64 transients per t_1 value, with 64 t_1 increments. The ^{1}H resonance assignments for the two glycine residues were based on ^{1}H{^{1}H} NOE results. The 2D ^{1}H–^{13}C correlated spectrum recorded from **3** was obtained using 64 t_1 values with 512 transients at each cycle. The relaxation delay was 2.5 s with a mixing time of 0.5 s for NOESY spectra. One-dimensional NOE experiments were performed in the difference mode where at least 256 transients were accumulated. The relaxation delay varied between 8 and 10 s, with a minimum required decoupler power to achieve a total saturation of the selected resonance line. The observe pulse was set to 90 deg with a spectral window of 4 kHz and 32 K data points. The concentrations were in the range of 1–3 mg/mL.

The determination of the temperature dependence of the chemical shifts was carried out in accordance with earlier descriptions for similar -Pro-Ser- containing model systems.[10] The amide proton chemical shifts are monitored over the range 10–40 °C in CD_3CN, in CD_3CN/H_2O (94:6), and in DMSO-d_6/CD_3CN (8:2). The temperature coefficients ($-\Delta\delta/\Delta T \times 10^3$ [ppm/K]) are reported in Table IX.

CD Measurement. All the CD measurements were performed on a Jobin-Yvon Mark V autodichrograph using circular quartz cells with

(20) Sheldrick, G. M. The structure-solution program SHELX-86, Institut für Anorganische Chemie der Universität, Göttingen, F.R.G.

(21) Frenz, B. A. and associates The program package SDP, Enraf-Nonius Corporation, Delft, Netherlands and Bohemia, New York, U.S.A.

Table VI. Data for the X-ray Diffraction Study of Cyclo[(δ)Ava-Gly-Pro-Ser(O^{t}Bu)-Gly]·2H$_2$O

(A) Crystal Data at 21 (1) °C

crystal system: monoclinic	$Z = 2$
space group: $P2_1$ [C_2^2; no. 4]	crystal size: 0.42 ×
a = 9.968 (3) Å	0.50 × 0.55 mm
b = 13.969 (7) Å	formula wt: 489.57
c = 10.175 (3) Å	ρ_{calc} = 1.255 g cm^{-3}
β = 113.88 (3)°	μ = 0.90 cm^{-1} (Mo K$\bar{\alpha}$)
V = 1295.5 (17) Å^3	

cell constant determination: 6 pairs of ±(hkl) and refined 2θ, ω, χ values in the range 25 ≤ |2θ| ≤ 27° (λ(Mo K$\bar{\alpha}$) = 0.71073 Å)

(B) Measurement of Intensity Data

radiation: Mo K$\bar{\alpha}$, graphite monochromator
reflections measured: +h,+k,±l (3 ≤ 2θ ≤ 50°)
scan type, speed: ω, vble, 2.44–5.33°/min
scan range: symmetrical, 1.0°; 1.0° background offset
no. of reflections measured: 2530; 2389 in unique set
standard reflections, period 100: 53$\bar{2}$; 063 reflections; variation ≤ ±3σ(I) for each
data reduction: as before[a]
statistical information: R_{av} = 0.011 (0kl reflections)

(C) Refinement

refinement,[a] with 1958 data for which $I > 1.96\ \sigma(I)$
weighting of reflections: as before,[b] p = 0.04
solution:direct methods (SHELXS-86)[3]
refinement:[c] full-matrix least-squares, with
anisotropic temperature factors for O, N, and C atoms;
isotropic temperature factors for refined H attached to N, O atoms and fixed H
attached to C atoms;
secondary extinction parameter, 7.3 (17) × 10^{-7};
R = 0.0401; R_w = 0.0447; SDU = 1.47;
R (structure factor calcn with all 2389 reflections) = 0.065
final difference map: one peak, 0.18 e$^-$/Å^3; random peaks ≤0.13e$^-$/Å^3; largest negative peak −0.19 e$^-$/Å^3

[a] Foxman, B. M.; Goldberg, P. L.; Mazurek, H. *Inorg. Chem.* **1981**, *20*, 4381. All computations in the present work were carried out using the ENRAF-NONIUS Structure Determination Package[4] and the direct methods program SHELXS-86.[3] [b] Corfield, P. W. R.; Doedens, R. J.; Ibers, J. A. *Inorg. Chem.* **1967**, *6*, 197. [c] $R_{av} = \sum|I - I_{av}|/\sum I$; $R = \sum||F_o| - |F_c||/\sum|F_o|$; $R_w = \{\sum w[|F_o| - |F_c|]^2/\sum w|F_o|^2\}^{1/2}$; SDU = $\{\sum w[|F_o| - |F_c|]^2/(m - n)\}^{1/2}$ where m (=1958) is the number of observations and n (=339) is the number of parameters.

path lengths of 0.01, 0.02, or 0.05 cm, with a sensitivity setting at 1 × 10^{-6}–1 × 10^{-5}. The response time setting for the spectrometer was 2 or 3 s, with data acquisition time of 5 s for the Apple IIe computer connected to the spectrometer, which ensured noise reduction as well as full-magnitude signal conversion from analogue to digital. Each measurement was the average result of five repeated scans in steps of 0.2 nm at 22 °C. The CD spectra of peptides were usually measured at 0.5 mg/mL, which is lower than that used for ^{1}H NMR acquisition (2–4 mg/mL). In order to achieve a direct comparison of the two types of conformational data, CD spectra were recorded in a wide concentration range, with extremes of 0.5 and 2.3 mg/mL. No significant concentration dependence has been observed, but the band intensities below 200 nm were slightly smaller at higher concentrations. For NMR comparison, the curves reported in Table X were used. For mean residue ellipticity calculation the molecular weights used were normalized to For-Aaa-Aaa-NH$_2$ as shown in Table XII.

CD Curve Analysis. Assuming the additivity of the chiral contributions of the different secondary structural elements the circular dichroism (CD) spectra of a peptide is therefore a function [$f(\lambda)$] which may be decomposed by a suitable method. If P is the number of the pure components and w_i is the conformational weight (%) of the ith pure component curve [$g_i(\lambda)$], the measured CD curve [$f^m(\lambda)$] can always be fitted by a calculated curve [$f^c(\lambda)$] which has the following form:

$$f^c(\lambda) = \sum_{i=1}^{P} w_i \cdot g_i(\lambda) \qquad (1)$$

A method solving such an equation has been developed earlier[34a,b] and called the CCA method. The sum of the weights of the pure components for a peptide must be equal to 1 (constraint a) with all weights being positive (constraint b). Peptides can be represented on a simplex, where the volume of the simplex should be minimal (constraint c). This algorithm uses only "natural constraints" (a, b, and c)[34a,b] and yields adequate pure component curves and weights, respectively. (For more details, see ref 34a,b.) An application is reported herein of the previously discussed

Table VII. Atomic Coordinates for Cyclo[(δ)Ava-Gly-Pro-Ser(O^{t}Bu)-Gly]·2H$_2$O[a,b]

atom	x	y	z	B (Å^2)
O1	−0.0021 (3)	−0.131	0.3432 (3)	6.41 (7)
O2	0.2757 (2)	−0.0018 (2)	0.6550 (2)	4.39 (5)
O3	0.5597 (3)	0.0489 (2)	1.0236 (2)	5.41 (6)
O4	0.9019 (2)	0.1006 (2)	0.9061 (2)	4.52 (6)
O5	0.5913 (3)	0.3173 (2)	0.7912 (3)	6.05 (8)
O6	0.2407 (2)	0.1856 (2)	0.4141 (2)	4.47 (5)
O7	−0.5231 (3)	−0.4157 (2)	−0.5120 (3)	5.61 (6)
O8	−0.5088 (3)	−0.4968 (2)	−0.2637 (3)	6.49 (7)
N1	0.1849 (3)	−0.0352 (2)	0.3686 (3)	4.25 (7)
N2	0.4545 (3)	−0.1110 (2)	0.7199 (3)	3.49 (6)
N3	0.6019 (2)	0.0600 (2)	0.8247 (2)	3.26 (5)
N4	0.4124 (3)	0.2077 (2)	0.7074 (3)	3.63 (6)
N5	0.0594 (3)	0.2715 (2)	0.4379 (3)	4.75 (8)
C1	−0.0575 (5)	0.2497 (3)	0.2981 (4)	5.6 (1)
C2	−0.1657 (4)	0.1784 (3)	0.3087 (4)	5.3 (1)
C3	−0.1017 (4)	0.0804 (3)	0.3591 (3)	4.48 (8)
C4	−0.0591 (4)	0.0273 (3)	0.2512 (4)	4.65 (9)
C5	0.0417 (4)	−0.0535 (3)	0.3233 (3)	4.10 (8)
C6	0.2948 (4)	−0.0969 (3)	0.4660 (3)	4.34 (8)
C7	0.3402 (3)	−0.0664 (2)	0.6216 (3)	3.56 (7)
C8	0.5026 (4)	−0.0886 (3)	0.8728 (3)	3.94 (8)
C9	0.6244 (5)	−0.1617 (3)	0.9448 (5)	7.0 (1)
C10	0.6268 (7)	−0.2248 (5)	0.8388 (6)	13.3 (2)
C11	0.5376 (4)	−0.1911 (3)	0.6955 (4)	5.3 (1)
C12	0.5552 (3)	0.0130 (3)	0.9115 (3)	3.31 (7)
C13	0.6621 (3)	0.1559 (2)	0.8548 (3)	3.40 (7)
C14	0.7945 (3)	0.1654 (3)	0.8188 (3)	3.87 (8)
C15	1.0041 (3)	0.0638 (3)	0.8516 (3)	4.33 (8)
C16	1.0779 (4)	0.1438 (4)	0.8063 (5)	7.2 (1)
C17	1.1122 (4)	0.0072 (4)	0.9735 (5)	7.9 (1)
C18	0.9235 (5)	−0.0017 (4)	0.7236 (5)	7.0 (1)
C19	0.5501 (3)	0.2337 (3)	0.7803 (3)	3.64 (7)
C20	0.2945 (3)	0.2734 (3)	0.6313 (4)	4.19 (8)
C21	0.1961 (3)	0.2387 (2)	0.4804 (3)	3.76 (7)
HO7A	−0.524 (3)	−0.435 (3)	−0.431 (3)	5.7 (8)
HO7B	−0.438 (4)	−0.378 (4)	−0.492 (5)	10 (1)
HO8A	−0.516 (4)	−0.481 (3)	−0.193 (4)	8 (1)
HO8B	−0.461 (5)	−0.555 (4)	−0.234 (5)	11 (2)
HN1	0.201 (3)	0.018 (2)	0.366 (3)	4.3 (7)
HN3	0.588 (3)	0.034 (2)	0.743 (3)	3.4 (7)
HN4	0.387 (2)	0.155 (2)	0.704 (3)	2.5 (6)
HN5	0.039 (3)	0.306 (3)	0.479 (3)	5.4 (9)

[a] Atoms refined using anisotropic temperature factors are given in the form of the isotropic equivalent displacement parameter defined as 1.33[$a^2B_{11} + b^2B_{22} + c^2B_{33} + ab\cos\gamma B_{12} + ac\cos\beta B_{13} + bc\cos\alpha B_{23}$]. [b] Numbers in parentheses in this and following tables are estimated standard deviations in the least significant digit.

Table VIII. Hydrogen Bonds in Cyclo[(δ)Ava-Gly-Pro-Ser(O^{t}Bu)-Gly]·2H$_2$O[a]

atoms X–H···Y	distance X···Y, Å	distance H···Y, Å	angle X–H···Y, deg	symmetry operation
N1–HN1···O6	3.134	2.39	165.6	x, y, z
N3–HN3···O7	2.972	2.28	137.0	$\bar{x}, {}^1/_2 + y, \bar{z}$
N4–HN4···O2	3.181	2.42	170.3	x, y, z
N5–HN5···O1	2.857	2.17	160.1	$\bar{x}, {}^1/_2 + y, 1 - z$
O7–HO7A···O8	2.720	1.86	168.8	x, y, z
O7–HO7B···O6	2.941	2.00	168.4	$\bar{x}, y - {}^1/_2, \bar{z}$
O8–HO8A···O3	2.764	1.98	171.6	$\bar{x}, y - {}^1/_2, 1 - z$
O8–HO8B···O5	2.757	1.85	165.7	$x - 1, y - 1, z - 1$

[a] O7 and O8 are the two oxygens of the two incorporated water molecules.

Table IX. Temperature Coefficients [$-\Delta\delta/\Delta T \times 10^3$ (ppm/K)] of the Amide NH Chemical Shifts of Cyclo[(δ)Ava-Gly[1]-Pro-Ser(O[t]Bu)-Gly[2]] (**2**) and Cyclo[(δ)Ava-Gly[1]-Pro-Ser(OH)-Gly[2]] (**3**) in Three Different Solvents

2	DMSO/CD_3CN 8:2	CD_3CN	CD_3CN/H_2O 94:6	**3**	DMSO/CD_3CN 8:2	CD_3CN	CD_3CN/H_2O 94:6
Gly1 (NH)	2.5	2.0	2.5	Gly1 (NH)	2.8	1.6	4.0
Ser (NH)	5.5	4.0	5.4	Ser (NH)	5.1	4.6	5.2
Gly2 (NH)	2.2	1.8	1.7	Gly2 (NH)	3.5	3.2	3.8
(δ)Ava (NH)	5.3	2.5	5.3	(δ)Ava (NH)	4.2	3.7	4.0

Table X. Circular Dichroism Parameters (λ nm, $[\phi]_M$) of Observed Spectra for Cyclo[(δ)Ava-Gly-Pro-Ser(O[t]Bu)-Gly] (**2**) and Cyclo[(δ)Ava-Gly-Pro-Ser(OH)-Gly] (**3**) in Three Different Solvents

	acetonitrile			water			TFE		
	c (mg/mL)	λ_{nm}	$[\theta]_M$[a]	c (mg/mL)	λ_{nm}	$[\theta]_M$[a]	c (mg/mL)	λ_{nm}	$[\theta]_M$[a]
2	0.85[b]	224	−5653	1.36	220	−6390	0.8	219	−10170
		203.7	−21985		207.5	−11300		202	−24230
		191.4	7002		187	10450			
3	2.38	222.6	−6090	1.85	220	−1920	1.04	219	−13030
		205	−12998		206.2	−2943		204	−21650
					188.5	1850		184	4888

[a] For mean residue ellipticity calculations the used molecular weights are in Table XII. [b] 2% of water was added.

Table XI. $^1H\{^1H\}$ NOE Percentages and Interproton Distances (Calculated and Measured) in Cyclo[(δ)Ava-Gly-Pro-Ser(O[t]Bu)-Gly] (**2**) and Cyclo[(δ)Ava-Gly-Pro-Ser(OH)-Gly] (**3**)

	2 NOE (%)[g]		**2** interproton dist (Å)				**3** NOE (%)[g]		**3** interproton dist (Å)	
			from X-ray		from[e] NOE in CD_3CN				from[f] NOE in CD_3CN	
irradiated H/observed H	CD_3CN	DMSO/CD_3CN 8:2					CD_3CN	DMSO/CD_3CN 8:2		
Gly1 (NH)/Gly 1 (H^α)	<1, 3	<1	2.5	3.0	3.2	2.7	6, 2	4, 1	2.25	2.6
/(δ)Ava (H^α)	n	3	2.1	3.4			4	3	2.4	
/(δ)Ava (H^β or H^γ)	2.5	2	2.7[d]	3.9	2.7		4	4	2.3	
Gly2 (NH)/Ser (NH)	6	2	2.5		2.6		n	n		
/Ser (H^α)	5	4	3.2		2.9		8	4	2.5	
/Gly 2 (H^α)	7, 3	3, n[c]	2.5	2.9	2.4	2.7	6, 2	2, 1	2.2	2.6
Ser (NH)/Gly 2 (NH)	4	4	2.5		2.7		n	n		
/Ser (H^α)	7.5	4	2.9		2.7		8[a]	4[a]	2.5	
/Pro (H^α)	4.5	3	3.4		2.7		6[a]	4[a]	2.3	
/Ser (H^β)	2	3	2.5	3.7	2.85		7	2[b]	2.1	
/Pro (H^δ)	n[h]	n	2.9	4.0			2	2[b]	2.6	
(δ)Ava (NH)/Gly2 (H^α)	6, <1	2, n[c]	2.4	2.9	2.4	3.2	4, 1	2, 1	2.4	3.0
/(δ)Ava (H^δ)	6	3	2.3	2.9	2.4		3	3	2.4	

[a] Tentative due to Pro(H^α) and Ser(H^α) overlapping. [b] Pro(H^δ) and/or Ser(H^β). [c] Overlapped with solvent peak. [d] Gly 1(NH) (δ)Ava (H^γ) distances. [e] $\sigma_{ref} = 0.50$ calculated as suggested previously[24a] from Gly_2. [f] $\sigma_{ref} = 0.48$ calculated as suggested previously[24a] from Gly_2. [g] NOE (%) = $\eta_i(j)\cdot 100$. [h] n = not found.

Table XII. The Ten Models Used for Circular Dichroism Curve Deconvolution

		MW	MW_{core}[a]	MW/MW_{core}
1	(Boc-Pro-Thr-NHMe)	329	242	1.36
2	(Boc-Val-Thr-NHMe)	331	244	1.36
3	(Boc-Leu-Thr-NHMe)	345	258	1.34
4	(Boc-Pro-Ser-NHMe)	315	229	1.38
5	(Boc-Val-Ser-NHMe)	317	230	1.38
6	(Boc-Gly-Ser-NHMe)	275	188	1.46
7	(Boc-Pro-D-Ser-NHMe)	315	229	1.34
8	(Boc-Val-D-Ser-NHMe)	317	230	1.38
9	(cyclo[(δ)Ava-Gly-Pro-Ser(O[t]Bu)-Gly])	453	229	1.99
10	(cyclo[(δ)Ava-Gly-Pro-Ser(OH)-Gly])	397	229	1.74

[a] For comparison and calculation the "core-moiety" of the different models was used (For-Aaa^1-Aaa^2-NH_2).

method for 10 peptides, where the fitting error of the measured and calculated CD spectra was minimized:

$$\{\sum_{j=1}^{N} f_j^m(\lambda) - \sum_{j=1}^{N} f_j^c(\lambda)\}^2 = \{\sum_{j=1}^{N} f_j^m(\lambda) - \sum_{j=1}^{N}\sum_{i=1}^{P} w_{ij} g_i(\lambda)\}^2 \rightarrow \text{minimized}$$

Molecular Dynamics Simulations. Energy minimizations and dynamics trajectory calculations for models were performed using CHARMM[22] within QUANTA (POLYGEN) on a Silicon Graphics work station computer. Structure minimization was achieved by starting from the X-ray determined conformation (as torsional constraints), and then the structures were fully relaxed. (For type II β-turn conformation, the "central" amide was also twisted.) Molecular simulation was performed involving heating, equilibration, and simulation steps. The simulation times were selected between 20 and 200 ps (at 300 K), starting from either type I or type II

(22) Brooks, B. R.; Bruccoleri, R. E.; Olafson, D. B.; States, D. J.; Swaminmathan, S.; Karplus, M. *J. Comput. Chem.* **1983**, *4*, 187.

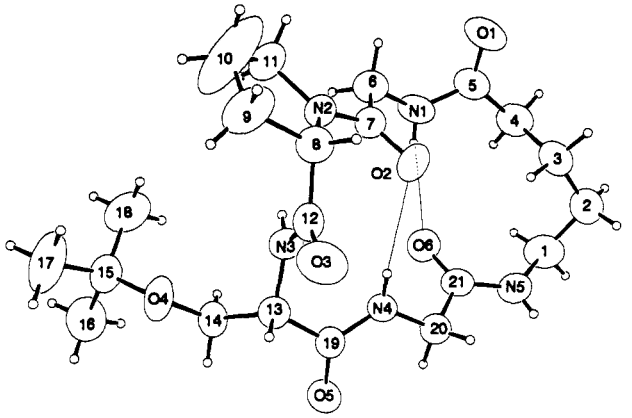

Figure 2. Molecular structure of cyclo[Gly-Pro-Ser(O'*Bu*)-Gly-(δ)Ava] (**2**) showing the two intramolecular H-bonds connecting the two glycine residues. Only carbon atoms are labeled with a single number.

conformations, and concluded when no significant variation of the conformationally allowed area was observed by increasing the simulation time.

Results and Discussion

Solid-State Conformational Analysis. The fact that crystals of **2** had been grown from the same solvent (CD_3CN) as that used for solution-state conformational investigations allowed an exact comparison. The molecular structure of **2** and the atomic numbering scheme are shown in Figure 2. Bond lengths and angles lie within normal ranges and are available as supplementary material. The analysis of the backbone torsion angles resulted in dihedral angles at the crucial hairpin moiety part $\phi_{Pro} = \phi_{i+1} = -63.34°$, $\psi_{Pro} = \psi_{i+1} = -23.18°$, $\phi_{Ser} = \phi_{i+2} = -96.24°$, $\psi_{Ser} = \psi_{i+2} = +4.77°$), which are rather close to the predicted values of a type I β-turn, with extended-like conformations at position *i* and *i*+3 ($\phi_{Gly1} = -92.85°$, $\psi_{Gly1} = -171.65°$, $\phi_{Gly2} = +135.25°$, $\psi_{Gly2} = +152.26°$). This "ideal type I" β-turn conformation in the crystalline state is found in a cyclic model, which, on the other hand, lacks the continuous system of amide chromophores of standard hexa- or pentapeptides obscuring the CD spectra of the β-turn. This crystal state conformation is not only very close to the expected values of an ideal type I β-turn[7] but also appears to be controlled mainly by intramolecular forces even in the crystalline state. The two intramolecular hydrogen bonds (see Table VIII and Figure 2) give additional rigidity to the whole backbone ring of the cyclopeptide, while the lone inter-ring H-bond may have minor effects on the backbone conformation (see Figure 3). Although the theoretically defined intramolecular H-bonds in antiparallel β-pleated sheets in proteins are usually shorter, the H-bond analysis on the basis of X-ray diffraction determined β-turn structures in proteins suggest that the 2.39 and 2.42 Å distances found herein (see Table VIII) fit perfectly within the normal range of NH···OC distances.[23a]

On the basis of a thorough investigation of X-ray diffraction-resolved protein structures, Wilmot and Thorton[23b] came to the conclusion that the ψ_{i+2} values are in some cases rather distorted from the predicted value; $\psi_{i+2} = 0°$. This observation agrees with theoretical calculations on model structures as well as with recently published X-ray data on Boc-Pro-Ser-$NHCH_3$.[10] From the connection between the presence of the 1 ← 4 intramolecular H-bond and the value of the ψ_{i+2} torsion angles it can be stated that the 1 ← 4 H-bond in β-turns is not a necessary requirement for the hairpin conformation, but stabilizes the structure when present. The identification of these intramolecular H-bonds will have a considerable role in the "structure extrapolation" from solid- to solution-state conformation.

Type I and type II β-turns differ from each other in the values of ψ_{i+1}, ϕ_{i+2}, and therefore the middle amide plane may have two orientations. In both conformations, this amide is roughly perpendicular to the cyclopeptide backbone ring. On the basis of CD, NMR, and molecular dynamics data on linear (-Val-Ser-, -Pro-Ser-)[9-12] and cyclic models (-Pro-Asn-, -Pro-Ala-),[24] these models were shown to mainly adopt these two conformations in various proportions. The mechanism for the interconversion of these two conformers is still not clear, but measurements have unambiguously reflected an equilibrium between type I and type II β-turn conformations in solution.[9-12,24] In contrast to the liquid- and gas-phase analysis, the crystalline conformation of **2** is a type I β-turn. Aside from the trivial explanation that the thermodynamically more stable type I conformation crystallizes, one can speculate that the two molecules of water per cyclopeptide incorporated in the crystal may have an important influence on the "conformation selection" (cf. Figure 4). The buildup of hydrogen bond networks (Figure 4) in the form of a water–water–amide polymer $(H_2O\cdots H_2O\cdots CONH-)_n$, interconnecting just the critical central amide groups, may have a crucial role in the determination of the conformation. This chain interaction, which is perpendicular to the intermolecular H-bonds, as shown in Figure 3, is further demonstrated in Figure 4. One fascinating aspect of the specific interaction between water molecules and the β-turn moiety is that in proteins the β-turns are usually on the surface, therefore exposed to the solvent. In order to investigate the precise role of water, a crystal of **2** was grown from anhydrous ethyl acetate under dried argon.[25] The crystallization was remarkably slower (30 days), but a cell constant and a space group determination demonstrated the identity of the two crystals. The experiment was repeated using ethyl acetate saturated with water, resulting in a *third* identical crystal. One can conclude that two water molecules (which interact with the backbone amide group connecting *i*+1 and *i*+2 residues according to the β-turn nomenclature) are incorporated regardless of the solvent or the amount of available water. Such a network, in which only the peptide backbone amides are involved in the H-bond interactions with neighboring water molecules, can serve as a "generalized" model, describing a possible way of type I β-turn solvation. It is of interest to note that α-helices in protein crystal structures have often been found to be hydrated, either by a water molecule hydrogen bonding to the backbone carbonyl oxygen atom or internally by inserting into the helix hydrogen bond and forming a hydrogen-bonded bridge between the backbone carbonyl oxygen and the amide nitrogen atoms.[38] It is probable that water may play a crucial role in the adoption of a single

Table XIII. The Coefficient Matrix Obtained by the Deconvolution of the Ten Circular Dichroism Spectra Measured in CH_3CN (for Curves See Figure 8)[c]

models[a]	1	2	3	4	5	6	7	8	9	10
comp 1[b]	23	5	0	18	7	30	0	50	35	54
comp 2[b]	76	80	83	55	66	63	22	0	63	46
comp 3[b]	1	15	17	27	27	08	78	50	2	0

[a] For numbering see Table XII. [b] For component curves see Figure 12A. [c] The weights of the calculated three pure component spectra are given in %.

Table XIV. The Coefficient Matrix Obtained by the Deconvolution of the Ten Circular Dichroism Spectra Measured in H_2O (for Curves see Figure 9)[c]

models[a]	1	2	3	4	5	6	7	8	9	10
comp 1[b]	0	0	17	16	12	14	81	97	30	46
comp 2[b]	37	61	63	0	47	18	0	3	70	22
comp 3[b]	63	39	20	84	41	68	19	0	0	32

[a] For numbering see Table XII. [b] For component curves see Figure 12B. [c] The weights of the calculated three pure component spectra are given in %.

(23) (a) Toniolo, C. *CRC Crit. Rev. Biochem.* **1980**, *9*, 1. (b) Wilmot, C. M.; Thorton, J. M. *Protein Eng.* **1990**, *3*, 479.

(24) (a) Stradley, S. J.; Rizo, J.; Bruch, M. D.; Stroup, A. N.; Gierasch, L. M. *Biopolymers* **1990**, *29*, 263. (b) Bruch, M. D.; Noggle, J. H.; Gierasch, L. M. *J. Am. Chem. Soc.* **1985**, *107*, 1400. (c) Noggle, J. H.; Schirmer, R. E. In *The Nuclear Overhauser Effect, Chemical Applications*; Academic Press: New York, 1974; p 1.

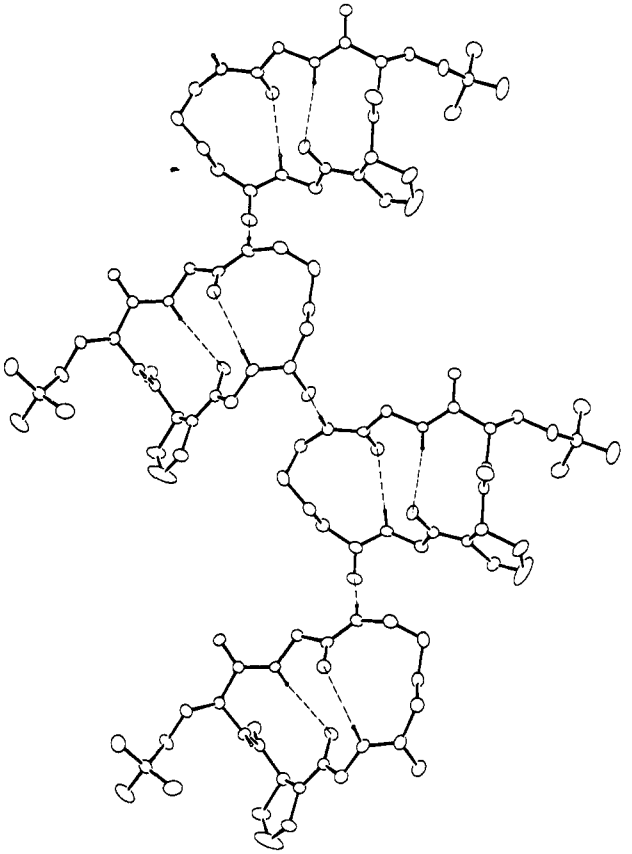

Figure 3. Intermolecular hydrogen bonding between molecules of cyclopeptide, cyclo[Gly-Pro-Ser(O^t*Bu*)-Gly-(δ)Ava].

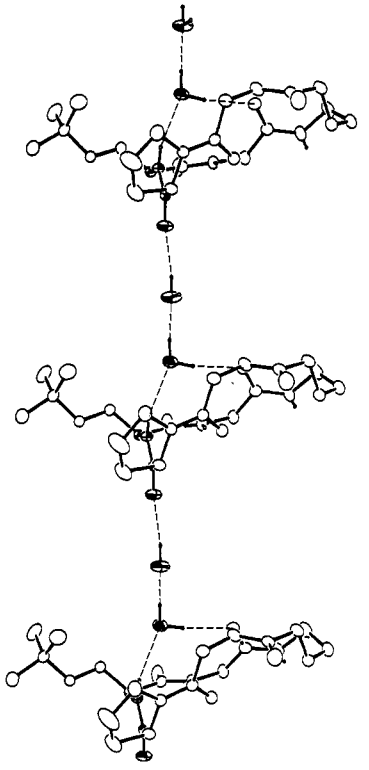

Figure 4. The intermolecular $(H_2O\cdots H_2O\cdots\text{–CONH–})_n$ hydrogen bond network in cyclo[Gly-Pro-Ser(O^t*Bu*)-Gly-(δ)Ava].

conformation in the solid state (namely the type I β-turn), but, as will be shown below, an additional conformer was observed in solution.

Solution-State Conformational Analysis. As demonstrated earlier by conformational studies in solution,[26] small peptides exist in an equilibrium mixture of several conformers, where the populations of the minima on the potential hypersurface are different. However, for some linear peptides, the population of a single conformer can be sufficiently high to enable assignment of its geometry unambiguously in a time-averaged measurement. As described earlier[27] for some linear models, such as Boc-Aaa-Ser-$NHCH_3$ (Aaa = Pro, Val), the conformational dominance of turn geometries has been determined.[27] It was shown by $^1H\{^1H\}$ NOE and $^1H\{^{13}C\}$ NOE measurements, that in aprotic hydrogen bond acceptor solvents (CD_3SOCD_3, CD_3CN) the main populated conformers were a mixture of a type I and a type II β-turn, along with a smaller amount of a "nontypical" backbone conformation. Cyclopeptides **2** and **3**, containing a β-turn structure in a bridged form, are in fact sterically restricted -Pro-Ser- β-turn models. In order to prove the similarity of the type I β-turn conformation in solid state and in solution, detailed H bond analysis was performed on **2** and **3** in CD_3CN.

Hydrogen Bond Analysis in Solution. The temperature dependence of the NH chemical shifts is the ^1H NMR technique most frequently used as an indicator of the existence of a hydrogen bond. In general, use of hydrogen bond acceptor solvents (DMSO, CH_3CN, H_2O, etc.) facilitates the interpretation of observed shifts.[7] Despite the fact that smaller values can suggest either intramolecular hydrogen bonding and/or the existence of an N–H proton unexposed to solvent, the presence of buried but not H-bonded amide protons is unlikely in **2** and **3**. The small temperature dependence measured herein for the NH resonances of two glycine residues for **2** in pure acetonitrile ($-\Delta\delta/\Delta T \times 10^3$ = 2.0, 1.8), in DMSO containing 20% of CH_3CN (2.2, 2.5) as well as in the presence of 6% water (1.7, 2.5) in CD_3CN, indicate the existence of two intra H bonds (cf. Table IX). In accordance with the H bond parameters found in the crystal, the measured ($-\Delta\delta/\Delta T$) values in three different solvents reflect the presence of H bonds in the solution conformation. The 1 ← 4 intramolecular hydrogen bond locks the conformation of the cyclic structure and with the second H bond the cyclopeptide becomes remarkably rigid. The second interchain backbone H bond ($NH_{Gly1} \rightarrow CO_{Gly2}$) is similar to those occasionally observed in globular proteins, when the β-turn is at "the middle" of an anti-parallel β-sheet (see Figures 1 and 2). Earlier FTIR data[9] suggested a similar interpretation of the H bond system.

When the serine side chain is unprotected, **3**, an additional H bond may occur between the side chain (–OH) and one of the amides of the backbone. An $NH \rightarrow O^\gamma H$ interaction was found in $(CH_3)_3C$-CO-Pro-Ser-$NHCH_3$,[11,12] but the lack of such an H bond was demonstrated in $(CH_3)_3C$-CO-O-Pro-Ser-$NHCH_3$.[10] Recent ab initio calculations suggested that the φ,ψ values of the serine backbone and the χ_1,χ_2 torsions of the side chain are coupled.[28] Therefore the appearance of a new H bond in **3** may modify the backbone conformation. The significant increase of the temperature coefficients of Gly_2 (NH) in **3** may reflect the decrease of the H bond strength, induced by such a side-chain backbone interaction. However values of $-\Delta\delta/\Delta T \times 10^3$, smaller than 4, are generally interpreted as a weak but significant participation of NH's in intramolecular H bonds.[7,24]

To have a second independent proof of the existence of the intramolecular H bonds in solution, the solvent dependence of the two glycine NH's was measured. The pure CD_3CN solution was "titrated" with H_2O up to the point at which the water dependence of the N–H's chemical shifts became linear (Figure 5). In **2** (cf. Figure 5) the water dependence of the chemical shifts of the two glycine's NH's was found to be linear and by contrast the NH's of the serine and the (δ)Ava residues which has a nonlinear region,

(25) Perrin, D. D.; Armarego, W. L. F. In *The Purification of Laboratory Chemicals*, 3rd ed.; Pergamon Press: 1988.
(26) (a) Dyson, J. H.; Rance, M.; Houghton, R. A.; Lerner, R. A.; Wright, P. E. *J. Mol. Biol.* **1988**, *201*, 161. (b) Wright, P. E.; Dyson, J. H.; Lerner, R. A. *Biochemistry* **1988**, *27*, 7167.
(27) Perczel, A.; Sándor, P.; Hollósi, M.; Fasman, G. D. *Biopolymers*, in press.
(28) Perczel, A.; Daudel, R.; Ángyán, J. G.; Csizmadia, I. G. *Can. J. Chem.* **1990**, *68*, 1882.

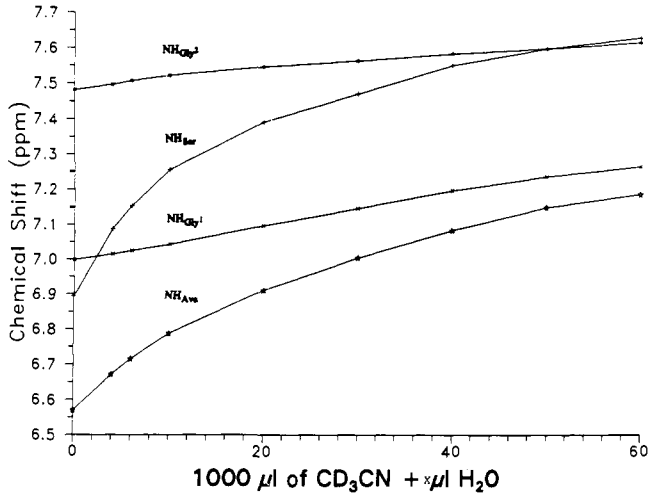

Figure 5. The NH chemical shifts dependence on the water content of cyclo[Gly-Pro-Ser(O'*Bu*)-Gly-(δ)Ava] in CD_3CN.

reflecting a basically different hydration pattern. The fitted analytical function,[29] in the form of $f(x) = k[1/(1-x)]$, yielded constants (k) values. The hydration procedure of the two glycine amide NH's was found to be basically different (different (k) values) than the solvation of the two other NH's in the cyclic peptides. The values of k for the two NH's of glycine residues were ten times smaller then those calculated for the NH's of serine and (δ)Ava, reflecting the smaller H bond affinity of the two glycine residues. Such differences were successfully correlated with intramolecular H bonds.

The solvent dependence and temperature coefficient of ^1H NMR measurements reported herein, together with earlier FTIR results[9] on **2** and **3**, suggest that the H bonds between the two glycine residues in solution are similar to those observed in the solid-state conformation. The strong steric restriction arising from the time-averaged presence of the two H bonds supports the idea that the global backbone conformation in solution may be only slightly different from the one measured in the crystal. However, the selective irradiation of the NH group of serine resulted in an enhancement of the H^{α}_{Pro} in **2** and **3** (cf. Table XI). This fact cannot be explained by assuming the unique presence of type I β-turn in solution. It has been demonstrated earlier using molecular mechanics[10,30,31] and molecular dynamics[24] simulations that the 360° rotation of the amide plane connecting residues $i+1$ and $i+2$ generally results in two minima, where the overall backbone geometry is close to type I or to type II β-turn conformations.

Conformation on the Basis of $^1H\{^1H\}$ NOE Data. As suggested by Dyson et al.,[26a] NOE experiments are useful measurements for the determination of the β-turn type.[32] However, using homonuclear correlated NOE information, only a type II β-turn can be assigned unambiguously. The enhancement of the H^{α} of residue $i+1$ induced by the selective irradiation of the NH of residue $i+2$ is indicative of a type II β-turn backbone conformation. By contrast there is no interproton distance shorter than 3 Å[7a] in a type I folded backbone geometry, which could be used as a marker for the unambiguous assignment of this conformation (see Figure 6). (The lack of an $^1H\{^1H\}$ NOE cannot be used as geometrical information.) Therefore the global assignment of a hairpin conformation can be performed on the basis of NOE data, but in a time-averaged measurement the individual determination

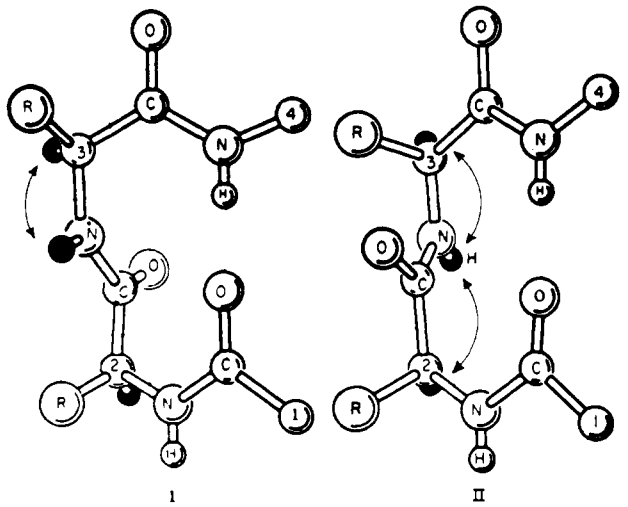

Figure 6. The marker distances in type I and type II β-turn conformations: distance$^{type\ I}$ (H^{α}_{i+1}–NH_{i+2}) = 3.5 Å, distance$^{type\ I}$ (H^{α}_{i+2}–NH_{i+2}) = 2.9 Å, distance$^{type\ II}$ (H^{α}_{i+1}–NH_{i+2}) = 2.1 Å, and distance$^{type\ II}$ (H^{α}_{i+2}–NH_{i+2}) = 2.3 Å.

of the different β-turn types using only NOE data will still be ambiguous.

NOESY spectra were recorded on **3** in CD_3CN to determine qualitatively whether the protons are spatially close (see Figure 7). The cross peaks indicate that the appropriate proton distances are shorter than 3 Å.[7a] The quantitative geometrical comparison between **2** and **3** is based on $^1H\{^1H\}$ NOE results performed in two different solvents (see Table XI). (DMSO is generally regarded as a strong H-bond acceptor; therefore a geometrical perturbation of **2** and **3** may occur by changing the pure CD_3CN to a DMSO/CD_3CN (8:2) solvent mixture.) However in both solvents the qualitative analysis of $^1H\{^1H\}$ NOE data (cf. Table XI) resulted in a similar structural assignment. Generally the observed enhancements are weaker in the "stronger" H bond acceptor (DMSO/CD_3CN) solvent, reflecting a larger conformational interconversion than is suggested in pure acetonitrile by NOE's. The distance of the proline α proton from the NH of serine in a type I β-turn conformation is at least 3.4 Å (cf. Table XI). However the irradiation of the serine's NH resulted in a definite enhancement in **2** and **3**, respectively, in both solvents. Not surprisingly the NOE data reflect the presence of an equilibrium mixture of the two major β-turns, as already suggested by Dyson et al.,[26a,b] Gierasch et al.,[24] and by others[10] for similar structures. In **2** the α proton of serine is more downfield-shifted than in **3**; therefore the identification of the observed enhancements on H^{α}_{Pro} and on H^{α}_{Ser} are evident. In **3** the α proton of the serine residue overlaps with the α proton of proline; therefore the quantitative NOE values are tentative. Although in **3** the overlap of the chemical shifts of H^{α}_{Pro} and H^{α}_{Ser} is the source of some ambiguity, the NOE enhancements in **2** and **3** reflect the simultaneous presence of the type II and type I β-turn. In spite of all efforts, the lack of any interproton distance marker specifically for a type I conformation results in an ambiguity in the quantitative determination of the pure conformational components even in these "rigid" structures. The sensitivity of CD spectroscopy, on the other hand, is such that it is uniquely capable of differentiating between type I and type II β-turns.[8a,b] The correlation between the herein reported NOE and CD spectra (both measurements were performed in the same solvent) present a unique opportunity to solve and determine the presence of a conformational mixture.

Interproton Distance Estimation Using Quantitative NOE Analysis. Using transient NOEs for similar cyclic peptides, Gierasch and co-workers[4a,b] pointed out that interproton distances may be determined as accurately as ±0.1 Å. Even though the suggested method is strictly correct only for two spin systems,[24a,b] it may result in a good approximation for multiple spins when the cross correlation between spins is negligible and a high irradiation

(29) Perczel, A.; Lengyel, I.; Fasman, G. D., manuscript in preparation.
(30) Némethy, G.; McQuire, J. R.; Pottle, M. S.; Scheraga, H. A. *Macromolecules* **1981**, *14*, 975.
(31) Zimmerman, S. S.; Pottle, M. S.; Némethy, G.; Scheraga, H. A. *Macromolecules* **1977**, *10*, 1.
(32) The use of the vicinal H–N–C^{α}–H proton coupling constants to distinguish between the two regions of ϕ_{i+2}(Ser) for type I (−90°) and for type II (80°) is not always adequate. According to Bystrov[37] the expected values of $^3J_{NH\alpha}$ for the corresponding torsion angles are highly similar (8 + 1 Hz). Therefore the identification of the β-turn type cannot be based only on $^3J_{NH\alpha}$ values only.

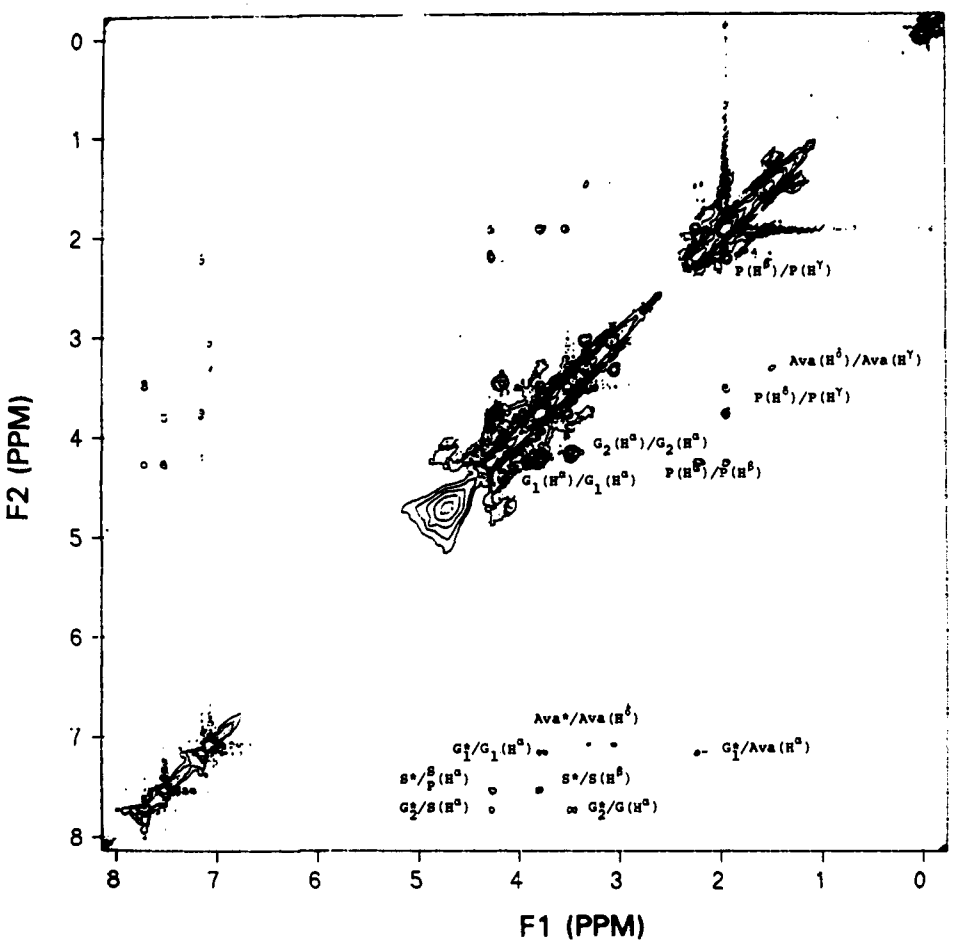

Figure 7. The 300-MHz NOESY spectra of cyclo[Gly-Pro-Ser(OH)-Gly-(δ)Ava] measured in CD_3CN using 0.5 s mixing time and 2.5 s of delay. The off-diagonal peaks are labeled where the downfield resonance is listed first.

power is used.[24c] If all dipolar interactions may be characterized by a single correlation time, then the ratio between two interproton distances (d_i and d_{ref}) is

$$\left(\frac{d_i}{d_{ref}}\right)^6 = \frac{\sigma_{ref}}{\sigma_i} \tag{2}$$

where σ_i and σ_{ref} are the individual cross-relaxation rates via dipole–dipole interaction.[33] As a reference value (σ_{ref}) the Gly^2 methylene interproton distance (d_{ref}) was used (which is 1.76 Å in the crystal state conformation) and was previously suggested to be 1.75 Å by Noggle and Schirmer.[24c] Comparing the calculated distances (obtained for **2** by such a calculation) to those measured in the crystal state, it can be concluded that some data correlates accurately: $d^{NOE}(Gly^2NH\text{-}SerNH)$ = 2.5 Å, $d^{X\text{-}ray}(Gly^2NH\text{-}SerNH)$ = 2.5 Å or $d^{NOE}(Gly^1NH\text{-}AvaH^\gamma)$ = 2.9 Å, $d^{X\text{-}ray}(Gly^1NH\text{-}AvaH^\gamma)$ = 2.7 Å. Other distances show significant deviation: $d_{NOE}(SerNH\text{-}ProH^\alpha)$ = 2.7 Å, $d^{X\text{-}ray}(SerNH\text{-}ProH^\alpha)$ = 3.4 Å. Deviations between NOE calculated and X-ray measured distances are larger in the β-turn moieties of the cyclic compounds than elsewhere, suggesting that two (or more) conformers interconvert rapidly. In fact this observation agrees quite well with the explanation given by Gierasch et al.[24a] for similar compounds. The calculated interproton distances on the basis of NOE percentages are therefore the weighted sum of those distances determined for the pure conformers. Theoretical calculations (MD) suggested that probably type I and type II β-turn backbone conformations are shared by **2** and **3**. In fact type I and type II β-turns are interrelated conformations, and each of these is not a rigid structure. Therefore the measured NOE distances can be interpreted by the following expression

$$\frac{1}{r_i^6} = \sum_{j=1}^{\text{all conf}} p_j \frac{1}{r_{ij}^6} \tag{3}$$

where p_j is the probability of the jth conformation in which the analyzed interproton distance is r_{ij}. Using the generally accepted interproton distances for type I {$d^{\text{type I}}(SerNH\text{-}ProH^\alpha)$ = 3.5 Å, $d^{\text{type I}}(SerNH\text{-}SerH^\alpha)$ = 2.9 Å} and for type II β-turns {$d^{\text{type II}}(SerNH\text{-}ProH^\alpha)$ = 2.1 Å, $d^{\text{type II}}(SerNH\text{-}SerH^\alpha)$ = 2.3 Å} and assuming that only the two above conformers are present, the population of the two β-turns can be estimated. Using the $SerNH\text{-}ProH^\alpha$ distances of $SerNH\text{-}SerH^\alpha$ distances resulted in a similar type of population; 18% of type II and 82% of type I β-turn. In the free OH containing model **3**, using the $SerNH\text{-}ProH^\alpha$ reference distance, 45% of type I β-turn and 55% type II β-turn were found, but using the $SerNH\text{-}SerH^\alpha$ reference distance resulted in 52% of type I β-turn and 48% of type II. Due to high sensitivity of the previous distances to ψ_{Pro} and ϕ_{Ser}, values with a 7% variation in conformational ratio are very reasonable.[24a,b]

Conformations in Vacuum. The conversion of the measured NOE percentages to interproton distances requires a reference distance (d_{ref}, see eq 1), which must be insensitive toward conformational changes. The interpretation of the calculated conformational percentages on the basis of quantitative NOE strongly depends on marker interproton distances in the "pure conformations". However, the pure conformers may differ from the "ideal conformers" (obtained from averaging several β-turns),

(33) The preirradiation time-dependence of the NOE difference spectra can be fitted to the following exponential function:[4a,24a,c]

$$\eta_i(j) = (\sigma_{ij} * T_{1i})^*[1 - \exp(-t/T_{1i})]$$

where σ_{ij} is the cross-relaxation rate via dipole–dipole interaction between spins i and j, and T_{1i} is the total relaxation time of spin i. If t is large enough in comparison to T_{1i}, the exponential term becomes negligible, and the previous equation will have the following form:

$$\eta_i(j) = \sigma_{ij}{}^* T_{1i}$$

The values of σ_{ij} were determined from this equation for distance calculations.

Chart I

	marker interproton dist	in the "ideal conf"	in the X-ray of **2**	in **2**	in **3**
type I β-turn	NH_{Ser}-H^{α}_{Ser}	2.9	2.9	2.9	2.8
	NH_{Ser}-H^{α}_{Pro}	3.5	3.4	3.4	3.5
type II β-turn	NH_{Ser}-H^{α}_{Ser}	2.3		2.3	2.3
	NH_{Ser}-H^{α}_{Pro}	2.1		2.3	2.3

resulting in alternative marker distances. However, the vacuum dynamic simulation yielded marker distances in the pure conformers that are in good agreement (±0.1 Å) with values obtained from X-ray measurements as well as with distances calculated from structure averaging (see Chart I). For molecular dynamics simulated structures see Figure 8.

This numerical resemblance proves on one hand that -Pro-Ser- dipeptides adopt β-turn conformations with high resemblance to the "ideal" hairpin geometry and confirms that the conformation marker distances used are valid. Two typical scatter plots, for a set of type I and type II β-turn backbone conformations, are shown in Figure 9. It was found that the global ring torsional angles were independent of the serine side chain (-O*t*Bu or -OH), resulting in similar allowed conformational regions for **2** and **3**. [Notice that the X-ray determined conformation for **2** falls perfectly within those highlighted areas (white arrows on Figure 9)], indicating that the conformation in the crystal is weakly or not perturbed by intermolecular H bonds and/or by other packing forces. On the time scale of the dynamics simulation (at 300 K in vacuum), no interconversion between the two backbone types was observed. Even though a simulation was made in vacuum, the two separated minimal energy conformers (type I and type II) for both **2** and **3** differ from each other by only a few kcal/mol (for example ΔE = 0.8 kcal/mol for **2**), suggesting a highly similar population of the above minima. This conformational separation of the similarly populated minima of **2** and **3** agrees with previous findings on -Pro-Ala- and -Pro-Asn- β-turn models,[24a] suggesting that even the most favorable and highly fixed hairpin models exhibit more than a single conformer in vacuum.

Solution Conformations on the Basis of CD Measurements. The CD spectra of **2** and **3** were measured in acetonitrile which is a weak hydrogen bond acceptor solvent, in 2,2,2-trifluoroethanol which has a strong proton donor capacity in H bond formation and in water which may be both donor and acceptor in an H bond system. The critical-point values of the spectra are summarized in Table X.

In Woody's theoretical approach,[8a,b] the class C CD spectra are expected to be similar to the α-helix spectra with weaker amplitudes; i.e., a negative $n \rightarrow \pi^*$ band around 220 nm and an exciton $\pi \rightarrow \pi^*$ couplet in the form of a negative band near 205 nm and a positive one below 200 nm. Usually such a spectrum is related to a backbone conformation similar to $(\phi = -60° \pm 30°, \psi = -30° \pm 30°)_n$ values. While the length of a helix (n is the number of subunits) has a significant influence on the intensities,[6a] α-helical fragments ($\phi = -54°, \psi = -45°$), 3_{10} helices ($\phi = -60°, \psi = -30°$)$_n$ and type I β-turns ($\phi_{i+1} = -60°, \psi_{i+1} = -30°, \phi_{i+2} = -90°, \psi_{i+2} = 0°$) are expected to result in class C CD spectra. However, up to the present, no such β-turn model has been synthesized in which an accurate solution-state conformation analysis resulted in the unequivocal proof that only a type I β-turn conformation was present. As in the case of cyclic peptides **2** and **3**, the minor conformer(s) (type II β-turn, etc.) were always present from different origins and influenced the position and the intensities of the bands of class C spectra. Therefore, the measured CD spectra are always the sum of two (or more) pure conformational prototypes (type I, type II β-turn, etc.) having different CD curves. By assuming the additivity of the chiral contribution of different conformers, a CD curve of such a conformational mixture is interpreted as

$$f_j(\lambda) = \sum_{i=1}^{n} x_{ij} g_i(\lambda) \qquad (4)$$

where n is the number of pure component spectra and x_{ij} is the contribution (or weight) of the pure component $g_i(\lambda)$ in the $f_j(\lambda)$ spectrum. By assuming only two pure conformational components (i.e., type I and type II β-turns) the use of such a linear combination of two pure component curves [$g_I(\lambda)$ and $g_{II}(\lambda)$] with different weights (x_{iI} and x_{iII}) has been successfully applied to describing the conformational properties of the -Val-Ser- β-turn models.[27]

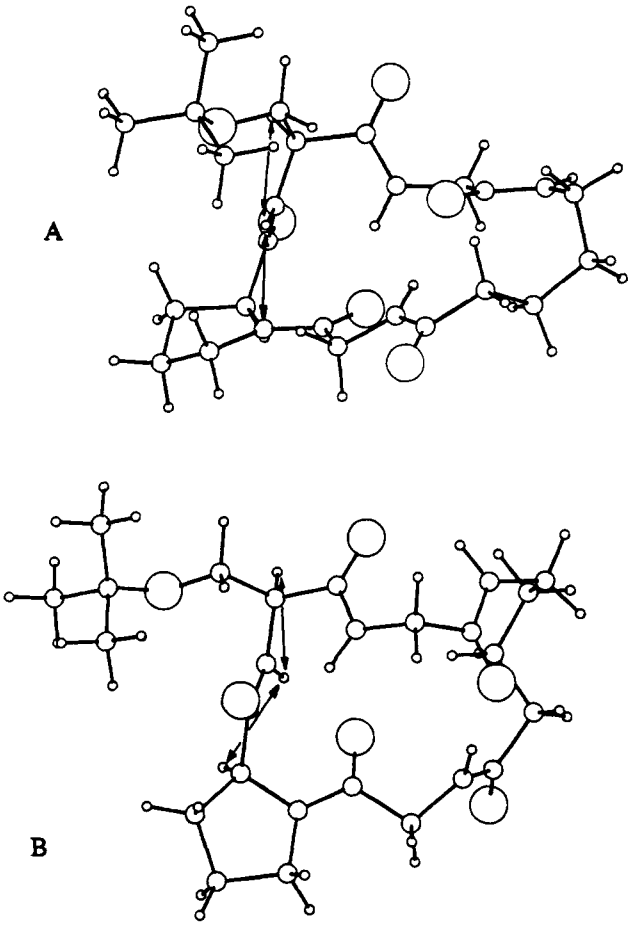

Figure 8. The two calculated minimal energy related structures according to molecular dynamics (A = type I β-turn and B = type II β-turn). The type I structure contains the same H bond pattern as was found in the crystal (cf. Figure 3), with slightly shorter H bond distances (NH_{Gly2}/CO_{Gly1} = 2 Å and NH_{Gly1}/CO_{Gly2} = 2.02 Å). The type II conformation is stabilized by three intramolecular H bonds (NH_{Ser}/CO_{Gly1} = 2 Å, NH_{Ava}/CO_{Ser} = 2.02 Å, and NH_{Gly1}/CO_{Gly2} = 1.92 Å).

As discussed earlier, it appears that even the most carefully designed β-turn model exhibits more than one conformation in solution. *Therefore the direct identification of the pure CD spectra of any β-turns, on the basis of a single model, is unlikely.* However, there is a way of solving such a problem on the basis of the measured CD spectra, which may be termed "conformation deconvolution". The extraction of the pure component [$g_1(\lambda)$, $g_2(\lambda)$,...] from a set of $f_j(\lambda)$ is a feasible procedure. {This algorithm, called Convex Constraint Analysis, functions conversely to a linear combination, aiming to determine the weights (x_{ij}) and the pure component curves [$g_i(\lambda)$] from a set of measured CD spectra [$f_j(\lambda)$]}. In order to carry out such a deconvolution the CD spectra of ten similar models have been collected (cf. Table XII and Figures 10 and 11); all contain only two chiral centers with a serine or threonine residue at position i+2. All spectra were recorded at 22 °C in CH_3CN (cf. Figure 10) and in H_2O (cf. Figure 11), respectively. The two data sets were analyzed separately using the recently developed algorithm called Convex Constraint Analysis.[34]

(34) (a) Perczel, A.; Tusnády, G.; Hollósi, M.; Fasman, G. D. *Protein Eng.* **1991**, *4*, 669. (b) Perczel, A.; Tusnády, G.; Hollósi, M.; Fasman, G. D. *Croatica Chim. Acta* **1989**, *62*, 189.

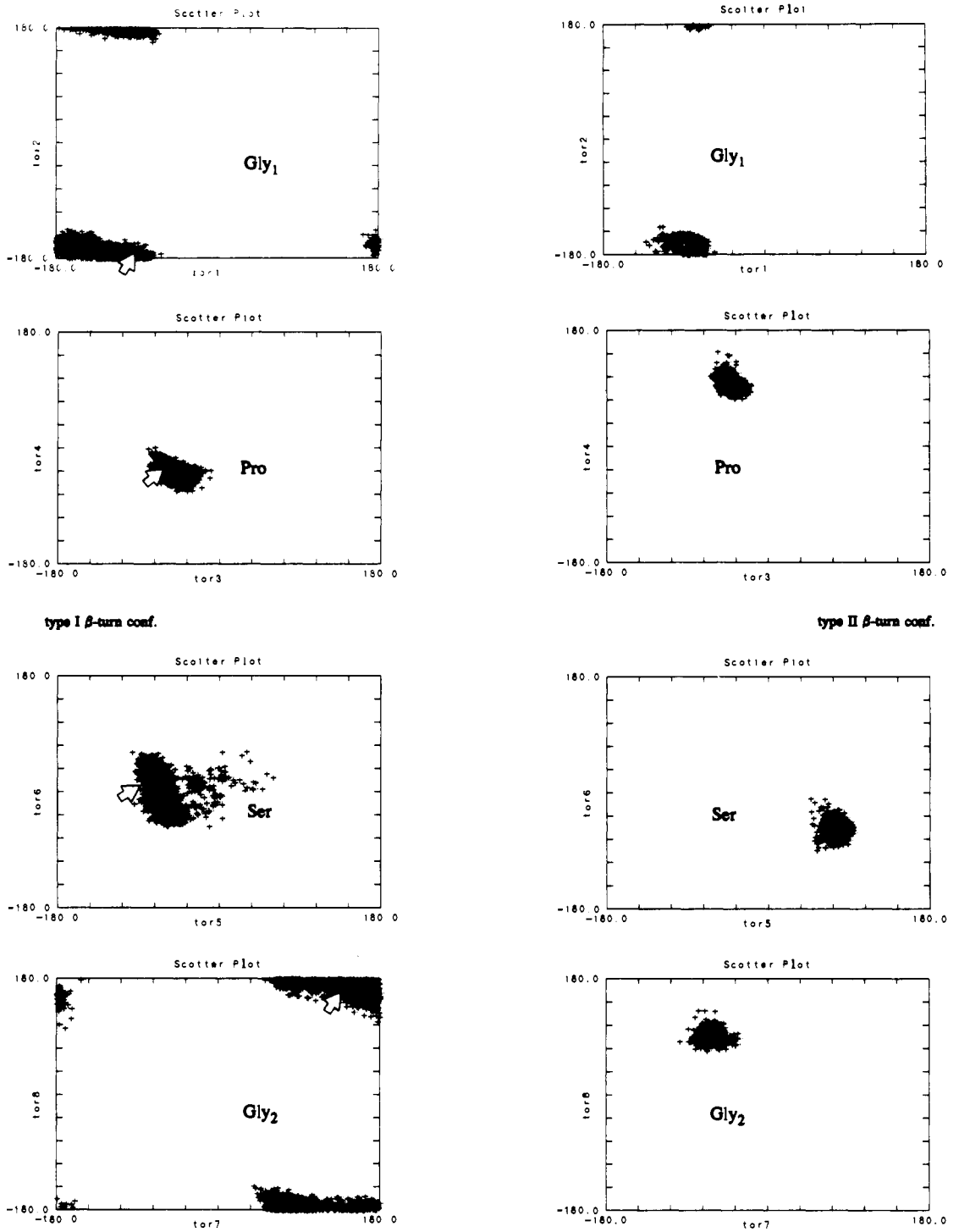

Figure 9. The allowed conformational area of the ϕ_i backbone torsional angles for cyclo[Gly_1-Pro-Ser(O^t*Bu*)-Gly_2-(δ)Ava] according to molecular dynamics vacuum simulation (300 K and 150 ps). White arrows point to observed backbone torsional angles using the X-ray diffraction data. Notice that no interconversion of type I and type II ring conformations was observed on the time scale of the dynamics animation. Conformational investigation of cyclo[Gly_1-Pro-Ser(OH)-Gly_2-(δ)Ava] resulted in identical ϕ_i and ψ_i areas.

The deconvolution into three pure component curves, of the CD spectra of ten selected turn models measured in CH_3CN, resulted in a relatively small standard deviation (dev = 2.04 molar ellipticity × 10^3).[34] The shape of the component spectra are shown in Figure 12A, and weights are given in Table XIII. All three pure component spectra in the aprotic hydrogen bond acceptor acetonitrile are blue-shifted (≈5–10 nm),[36] reflecting the well-known fact that the electron transition (n → π*, π → π*) energies are different in CH_3CN than in H_2O.

On the basis of literature data, component 1 (cf. Figure 12A) shows a high resemblance to class B[8a,b] CD spectra, usually related to a type II β-turn conformation in -L-Aaa-L-Aaa- or -L-Aaa-Gly-containing models. Component spectrum 2 is similar to class C spectra correlated previously with type I β-turn geometry. The third pure component (component 3) is very similar to a class C′ spectrum which has never been unambiguously correlated with any hairpin conformation but has been observed in -L-Aaa-D-Aaa-

(35) Ten spectra were digitized at each nanometer in the range of 185–260, and the standard deviation was determined as above:

$$\mathrm{dev}^2 = \sum_{j=1}^{10}[f_j^{\mathrm{measd}}(\lambda) - \sum_{i=1}^{3} x_{ij} * g_i(\lambda)]^2$$

(36) Wetlaufer, D. B. *Adv. Prot. Chem.* **1962**, *17*, 304.

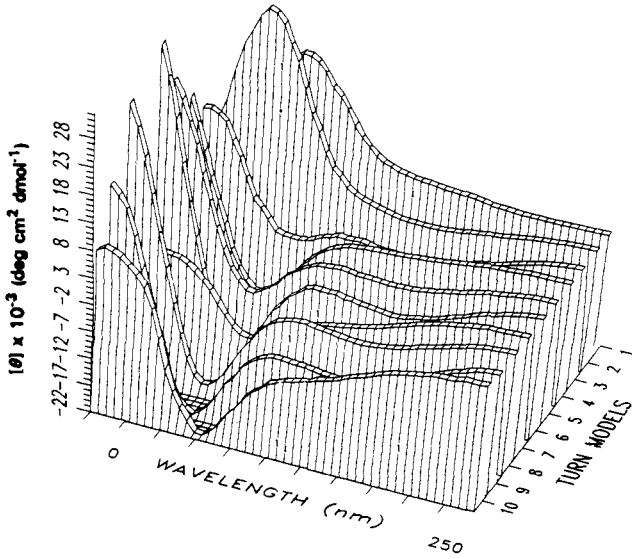

Figure 10. Circular dichroism spectra of ten β-turn models measured in acetonitrile at 22 °C in the concentration range of 0.5–2 mg/mL using a 0.2-mm path length cell. (See for details refs 9, 10, and 27): 1 (Boc-Val-D-Ser-NHMe), 2 (Boc-Pro-D-Ser-NHMe), 3 (Boc-Pro-Ser-NHMe), 4 (Boc-Gly-Ser-NHMe), 5 (Boc-Val-Ser-NHMe), 6 (Boc-Leu-Thr-NHMe), 7 (cyclo[(δ)Ava-Gly-Pro-Ser(OH)-Gly]), 8 (Boc-Val-Thr-NHMe), 9 (Boc-Pro-Thr-NHMe), and 10 (cyclo[(δ)Ava-Gly-Pro-Ser(O'Bu)-Gly]).

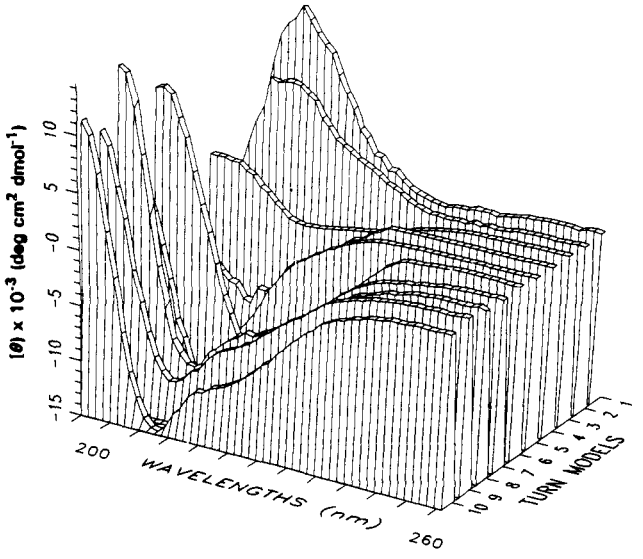

Figure 11. Circular dichroism spectra of ten β-turn models measured in H_2O at 22 °C in the concentration range of 0.5–2 mg/mL using a 0.2-mm path length cell. (See for details ref 9, 10, and 27): 1 (Boc-Val-D-Ser-NHMe), 2 (Boc-Pro-D-Ser-NHMe), 3 (cyclo[(δ)Ava-Gly-Pro-Ser(OH)-Gly]), 4 (Boc-Pro-Ser-NHMe), 5 (Boc-Gly-Ser-NHMe), 6 (cyclo[(δ)Ava-Gly-Pro-Ser(O'Bu)-Gly]), 7 (Boc-Pro-Thr-NHMe), 8 (Boc-Leu-Thr-NHMe), 9 (Boc-Val-Ser-NHMe), and 10 (Boc-Val-Thr-NHMe).

models[13,15,27] adopting mainly a type II β-turn. This assignment agrees with values in the coefficient matrix (Table XIII) showing that the C'-like pure component spectrum (component 3 on Figure 12A) is dominant only in the spectra of -L-Aaa-D-Aaa- models (78% in Boc-Pro-D-Ser-NHMe and 50% in Boc-Val-D-Ser-NHMe) and has only a minor contribution elsewhere. On the basis of $^1H\{^1H\}$ NOE measurements reported earlier,[27] Boc-Pro-Ser-$NHCH_3$ (**4**) and Boc-Val-Ser-$NHCH_3$ (**5**) predominantly exhibit a conformational mixture of type I and type II β-turns. Values obtained by deconvolution reflect the above observations, yielding 45% and 34% of type II conformation.

The interpretation of the conformational mixture of **2** in CH_3CN on the basis of CD is similar to one based on NMR results; in addition to the 35% of type II conformation, the dominant type I has a weight of 63%. This is in qualitative agreement with the quantitative NOE analysis which resulted in 80% and 20%, respectively. NOE data suggest for **3** (cf. Table XI) the quasi-equal contribution of type I and type II conformers (48.5% of type I and 51.5% of type II form). The drastic decrease of the CD band intensities (see for Table X) compared to those of **2** is in itself indicative of such a conformational mixture on the basis of previous results.[27] The deconvolution resulted in weights (46% of type I and 54% of type II) which are in excellent agreement with NOE data and furthermore suggests that in CH_3CN **3** *is present* in a quasi-equal ratio of the *two forms*. The increase of the type II β-turn percentage in **3** compared to the side-chain protected compound **2** may be related to the appearance of an additional H bond formation between the serine side chain and the NH of the backbone.

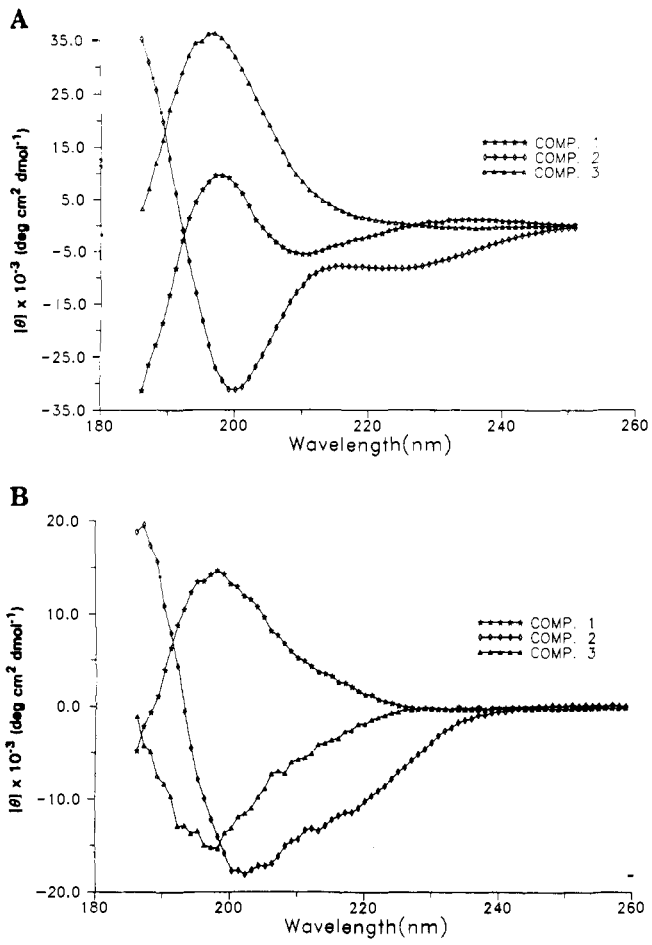

Figure 12. The three pure component curves obtained by deconvolution of the circular dichroism curves of ten selected β-turn models: (A) in CH_3CN and (B) in H_2O.

CD spectra measured in water were deconvoluted into three pure component spectra, where the standard deviation was small (dev = 0.73 molar ellipticity × 10^3), although the spectra measured in water gave a lower signal-to-noise ratio than those recorded in acetonitrile. Monitored by CD, the cleavage of the *tert*-butyl-ether from **2** resulted in a drastic decrease in the band intensities of **3**, even though the positions of the maxima and minima remained the same (cf. Table X and Figure 12B). The decrease of band intensities arises not from "optical impurity" but from an increase of conformational mobility. By introducing another "bulky" side-chain protecting group (tetrahydropyranyl ether) the side-chain mobility decreased, influencing the backbone conformations, which was monitored by the increase of the band intensities (cf. Figure 13). As suggested earlier, the free OH group of the serine residue may play an important role in the stabilization of a β-turn through specific backbone side-chain interaction. The substitution of the $-CH_2OH$ group of the serine residue by an

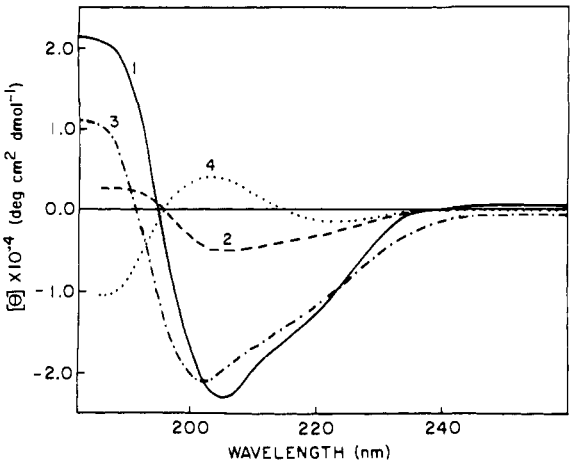

Figure 13. The CD spectra of four cyclo[Gly-Pro-Yyy-Gly-(δ)Ava] in water, where 1, Yyy=Ser(O'Bu); 2, Yyy=Ser(OH); 3, Yyy=Ser(OThp); and 4, Yyy=Gly.

H (glycine residue) further influenced the conformational equilibrium (cf. Figure 13, curves 2 and 4). The herein reported chiroptical property changes of the identical backbone, induced by side-chain modifications, are rather similar to data obtained earlier, when similar CD curve interconversion was found to be proportional to the different ratios of type I and type II β-turn in a conformational mixture.[27] The above spectral changes (cf. Figure 13, curves 1 to 4) suggest that in the side-chain protected serine samples, the class C type spectrum dominates (curves 1 and 3), but in cyclopeptides with a free serine OH group or without any side chain (glycine residue) the class B type spectrum becomes dominant. [It is proposed that all these spectra (cf. Figure 11 and Figure 13) are the conformational mixtures of the same CD prototypes but with different weights.]

The quantitative conformational analysis of the CD spectra of the ten selected β-turn models in water resulted in two similar component curves to those found in acetonitrile, i.e., class C and class C′, with slightly red-shifted spectral parameters. [In component spectrum 2 the shoulder calculated at 219 nm reflects a slightly blue-shifted n → π* transition with a higher amplitude than that determined in acetonitrile (cf. Figure 12)]. The major difference between the two sets of pure component spectra is in component 3. In water (Figure 12B) this spectrum has a single minimum below 200 nm which in small peptides is usually correlated with the "open" or "nontypical" backbone conformation. In fact this conformer has a major role in the linear -L-Aaa-L-Aaa- models (cf. Table XIV), where hydration may perturb the basic conformations. For the side-chain protected cyclopeptide model **2**, deconvolution resulted in rather similar conformational percentages (30% of type II and 70% of type I β-turns) to those found in acetonitrile (35% of type II and 63% of type I β-turns). In model **3**, the presence of a third conformation is probable besides these two pure conformers. The appearance of the side-chain OH group of the serine residue may stabilize the backbone conformation through a "nontypical" intramolecular H bond. As suggested by the qualitative CD curve interpretation, deconvolution shows that model **3** contains a significantly higher (46%) amount of the type II β-turn than found in model **2** (30%), due to the free OH group.

Conclusions

The unusual opportunity afforded by the crystallization and X-ray diffraction analysis of compound **2** from the same solvent, acetonitrile, in which a detailed solution-state conformation analysis was possible, minimized the error when conformation data were integrated. In the crystal, model **2** adopts an ideal type I β-turn structure with backbone torsion angles rather close to the data collected from X-ray structure analysis of globular proteins. In addition, the water molecules in the crystal structure bind specifically around the central amide plane of the β-turn, which may suggest a definite hydration pattern of β-turns in proteins. Using NOESY and $^1H\{^1H\}$ NOE data the type I β-turn conformation of models **2** and **3**, in acetonitrile, was found to be very similar, if not identical, to the conformation found in the solid state. Despite the fact that a single conformation of model **2** was obtained by crystallization, in solution an additional minor conformer (type II β-turn) was determined by $^1H\{^1H\}$ NOE measurements. The difference between the two conformations is that one amide plane is rotated by 160°, while all others are similarly oriented.

On the basis of MD calculations, the two types of β-turn differ only by a few kcal/mol. Therefore, it is not surprising that the thermodynamically more stable form may crystallize, but as a function of varying side chain, solvent, temperature, etc., both forms are present in solution with different ratios. Until recently, all the reported β-turn models consisted of more than a single conformer in all solvents; perhaps the "ideal" β-turn models do not exist. As found for **2**, even if the structure exhibits a single and "ideal" type I β-turn conformation in the crystal, in solution the appearance of one or more additional conformers are always detected. Therefore the identification of the CD and NMR properties of either of the two major pure β-turns (type I and type II) on the basis of a single model compound was not possible.

Using a recently developed algorithm (CCA), the conformational deconvolution of the CD curves of ten selected β-turn models was performed. The shape of the type I component curves (class C) in both solvents (acetonitrile and water) were similar and agreed with literature expectations (cf. Figure 12A,B). The ratio of the calculated percentages of type I and type II β-turns, on the basis of their CD spectra, was compared with conformational weights obtained from selective homonuclear NOE data.

Quantitative nuclear Overhauser effect measurements yielded interproton distances, which were compared to values determined by X-ray diffraction, and conformational ratios of **2** and **3**. For the first time NOE determined conformational weights were compared to the results of a quantitative CD interpretation. The backbone conformational changes induced by removing a side-chain protecting group (**2** → **3**) was successfully monitored by CD and NOE experiments, where the two methods yielded very similar conformational interconversion. The pure CD component curves of the two major β-turn types were determined and confirmed by NOE measurements. These data can now be used for rapid and precise conformational determinations of globular proteins using CD spectroscopy.

Registry No. 1, 136617-47-5; cyclo-**1**·2H_2O, 136642-55-2; **2**, 136617-48-6; **3**, 136617-49-7.

Supplementary Material Available: Tables S-I to S-V of bond lengths and angles, atomic displacement parameters, atomic coordinates for hydrogen atoms, and torsion angles (12 pages); table of observed and calculated structure amplitudes (9 pages). Ordering information is given on any current masthead page.

(37) Bystrov, V. F. *Prog. NMR Spectrosc.* **1976**, *10*, 41.
(38) Sundaralingham, M.; Sekharudu, Y. C. *Science* **1989**, *244*, 1333.